British Journal of Pharmacology

DOI:10.1111/j.1476-5381.2011.01594.x
www.brjpharmacol.org

RESEARCH PAPER

cAMP signalling protects proximal tubular epithelial cells from cisplatin-induced apoptosis via activation of Epac

Yu Qin[1], Geurt Stokman[1], Kuan Yan[2], Sreenivasa Ramaiahgari[1], Fons Verbeek[2], Marjo de Graauw[1], Bob van de Water[1] and Leo S Price[1]

[1]*Division of Toxicology, Leiden/Amsterdam Center for Drug Research, Leiden University, Leiden, the Netherlands, and* [2]*Section Imaging and Bioinformatics, Leiden Institute of Advanced Computer Science, Leiden University, Leiden, the Netherlands*

Correspondence
Dr Leo S Price, Division of Toxicology, Leiden/Amsterdam Center for Drug Research, Leiden University, Einsteinweg 55, P.O. Box 9502, 2300 RA Leiden, the Netherlands. E-mail: lsprice@lacdr.leidenuniv.nl

Keywords
cAMP signalling; Epac–Rap activation; cell–cell junction; cell apoptosis; cisplatin nephrotoxicity; proximal tubular epithelium

Received
3 February 2011
Revised
3 June 2011
Accepted
23 June 2011

BACKGROUND AND PURPOSE

Nephrotoxicity is the principal dose-limiting factor for cisplatin chemotherapy and is primarily associated with proximal tubular epithelial cells, including disruption of cell adhesions and induction of apoptosis. Cell adhesion and survival is regulated by, amongst other factors, the small GTPase Rap and its activator, the exchange protein directly activated by cAMP (Epac). Epac is particularly enriched in renal tubule epithelium. This study investigates the cytoprotective effects of cAMP–Epac–Rap signalling in a model of cisplatin-induced renal cell injury.

EXPERIMENTAL APPROACH

The Epac-selective cAMP analogue 8-pCPT-2′-O-Me-cAMP was used to activate the Epac–Rap signalling pathway in proximal tubular epithelial cells. Cells were exposed to cisplatin, in the presence or absence of 8-pCPT-2′-O-Me-cAMP, and nephrotoxicity was determined by monitoring cell–cell junctions and cell apoptosis.

KEY RESULTS

Activation of Epac–Rap signalling preserves cell–cell junctions and protects against cell apoptosis of mouse proximal tubular cells during cisplatin treatment. Activation with the Epac-selective cAMP analogue 8-pCPT-2′-O-Me-cAMP or receptor-mediated induction of cAMP both induced cytoprotection against cisplatin, whereas a PKA-selective cAMP analogue was not cytoprotective. 8-pCPT-2′-O-Me-cAMP mediated cytoprotection was blocked by RNAi-mediated silencing of Epac–Rap signalling in these cells. In contrast, 8-pCPT-2′-O-Me-cAMP did not protect against cisplatin-induced cell death of cancer cells that lacked Epac1 expression.

CONCLUSIONS AND IMPLICATIONS

Our study identifies activation of Epac–Rap signalling as a potential strategy for reducing the nephrotoxicity associated with cisplatin treatments and, as a result, broadens the therapeutic window of this chemotherapeutic agent.

Abbreviations

8-pCPT-2′-O-Me-cAMP, 8-(4-chlorophenylthio)-2′-O-methyladenosine-3′,5′-cyclic monophosphate; AM, acetoxymethyl ester; AMC, 7-amino-4-methylcoumarin; cisplatin, *cis*-diammineplatinum(II) dichloride; CREB, cAMP response element binding protein; Epac, exchange protein directly activated by cAMP; GEF, guanine nucleotide exchange factor; GFP, green fluorescent protein; HPRT, hypoxanthine phophoribosyltransferase; IM-PTEC, conditionally immortalized proximal tubular epithelial cells; NHE3, Na^+/H^+ exchanger 3; PSA, penicillin/streptomycin/amphotericin B; ZO-1, zona occludens-1

Introduction

Cisplatin has been widely used for clinical treatment of testicular cancer (Bosl and Motzer, 1997), ovarian carcinomas (Jandial *et al.*, 2009), head and neck cancer (Khuri *et al.*, 2000), malignant melanoma (Atzpodien *et al.*, 2007), lung cancer (Winton *et al.*, 2005) and breast cancer (Decatris *et al.*, 2004). However, severe adverse effects, in particular acute renal failure, limit the dose that can be given and consequently prevent more efficient treatment with higher doses (Nagai *et al.*, 1996; Mathe *et al.*, 2011). The principal cause of cisplatin-induced nephrotoxicity is direct damage to the proximal tubular epithelial cells (Townsend *et al.*, 2003; Vickers *et al.*, 2004). Physiologically, these cells are highly polarized, and their function is dependent on the integrity of cell adhesions and the actin cytoskeleton network (Mays *et al.*, 1995; Drubin and Nelson, 1996). The pathological alteration of these cells by cisplatin begins with disruption of cell adhesion and actin cytoskeleton reorganization, followed by depolarization and mislocalization of Na^+/K^+-ATPase. These changes eventually lead to cell detachment and/or cell death (Thadhani *et al.*, 1996; Imamdi *et al.*, 2004; de Graauw *et al.*, 2005). Cell–cell and cell–matrix adhesions provide epithelial cells with the environmental signals necessary to maintain normal cellular processes including cell survival, whereas loss of cell adhesion has been found to induce cell death through apoptosis (Meredith and Schwartz, 1997; Cordes, 2006). Although enhanced adhesion signalling may confer resistance of cancer cells to chemotherapeutic agents (Hodkinson *et al.*, 2007), it also represents a potential strategy for reducing toxicity in healthy tissues such as the kidney.

cAMP is a ubiquitous second messenger that is generated via the activation of the plasma membrane-bound or soluble adenylate cyclase. Several GPCRs increase intracellular cAMP levels via the activation of adenylate cyclase. Endogenous cAMP signalling regulates many cellular processes mostly through activation of PKA and the exchange protein directly activated by cAMP (Epac) (Cheng *et al.*, 2008). Epac is a guanine nucleotide exchange factor (GEF) for the small GTPase Rap (de Rooij *et al.*, 1998; Kawasaki *et al.*, 1998), a regulator of both integrin-mediated cell adhesion (Caron *et al.*, 2000; Reedquist *et al.*, 2000; Enserink *et al.*, 2004) and cadherin-mediated cell adhesion (Knox and Brown, 2002; Hogan *et al.*, 2004; Price *et al.*, 2004). Two isoforms, Epac1 and Epac2, are expressed at varying levels in different tissues. Epac1 is highly abundant in adult kidney, being particularly enriched in tubule epithelium, suggesting a functional role for Epac–Rap signalling (Kawasaki *et al.*, 1998; Honegger *et al.*, 2006; Ulucan *et al.*, 2007). Recent studies on the crystal structure of Epac proteins suggested that cAMP binding induces conformational changes of Epac proteins, thus lifting an autoinhibition of Epac to allow the binding and thus activation of Rap (Rehmann *et al.*, 2006; 2008).

cAMP analogues, such as 8-pCPT-2′-O-Me-cAMP, have been identified that selectively activate Epac without influencing the PKA pathway (Enserink *et al.*, 2002; Holz *et al.*, 2008). The conjugation of an acetoxymethyl ester (AM) to 8-pCPT-2′-O-Me-cAMP generates the membrane permeable analogue 8-pCPT-2′-O-Me-cAMP-AM, which accumulates intracellularly due to esterase-mediated cleavage of the AM group, reaching high cellular concentrations (Vliem *et al.*, 2008). These have been used to demonstrate that Epac–Rap signalling controls adhesion-associated processes including migration and survival (Kwon *et al.*, 2004; Lyle *et al.*, 2008) and mediates actions of cAMP-elevating G_s-coupled GPCRs (Enserink *et al.*, 2004; Holz *et al.*, 2008). An Epac-selective cAMP analogue was also used to demonstrate that Epac mediates cAMP-dependent regulation of the Na^+/H^+ exchanger 3 (NHE3) in mouse proximal tubules (Honegger *et al.*, 2006). We propose that the activation of Epac–Rap signalling in the kidney may promote cell adhesions and survival and consequently prevent cisplatin-induced nephrotoxicity.

In this study, we have investigated the effects of Epac activation in a model of cisplatin-induced nephrotoxicity. We showed that Epac activation by 8-pCPT-2′-O-Me-cAMP stabilized cell–cell junctions and protected against apoptosis of mouse proximal tubular epithelial cells in response to cisplatin treatment but did not protect Epac-deficient cancer cells from cisplatin-induced cell killing. Pharmacological activation of the Epac–Rap signalling pathway is therefore a potential strategy to reduce the nephrotoxicity and consequent renal insufficiency caused by cisplatin in clinical cancer treatment.

Methods

Isolation and culturing of cells

All animal care and experimental procedures complied with institutional guidance and national health standards and were approved by the Animal Care and Use Committee of Leiden University, the Netherlands. Eight-week old wild-type male C57BL/6 mice were purchased from Charles River (Maastricht, the Netherlands) and maintained at the animal facility of the Leiden University Gorlaeus Laboratories.

Mice were anaesthetized by i.p. injection of Euthasol (20%, ASTfarma, Oudewater, the Netherlands). Kidneys were minced and digested with collagenase Type XI (0.6 $g \cdot L^{-1}$, 2330 units$\cdot mg^{-1}$ of collagen digestion activity) in HBSS (137 mM NaCl, 5 mM KCl, 0.8 mM $MgSO_4$, 0.4 mM Na_2HPO_4, 0.4 mM KH_2PO_4, 1.3 mM $CaCl_2$, 4 mM $NaHCO_3$, 25 mM HEPES, 5 mM D-glucose, pH 7.4) for 30 min at 37°C. The cell suspension was washed for three times in HBSS. After the washing steps, cells were re-suspended in Dulbecco's modified Eagles medium (DMEM)/Ham's F12 (1:1) (Invitrogen) containing 1% (v/v) fetal bovine serum (FBS, Hyclone, Etten-Leur, the Netherlands), 0.5 $mg \cdot mL^{-1}$ BSA, 10 $ng \cdot mL^{-1}$ epidermal growth factor, 10 $ng \cdot mL^{-1}$ cholera toxin, 50 nM hydrocortisone, 15 mM HEPES, 2 mM glutamine (Invitrogen), 5 $\mu g \cdot mL^{-1}$ insulin and transferrin, 5 $ng \cdot mL^{-1}$ sodium selenite (Roche Applied Science, Mannheim, Germany) and 1% (v/v) penicillin/streptomycin/amphotericin B (PSA, Invitrogen). Cells were maintained at 37°C in a humidified atmosphere of 95% air/5% CO_2, and medium was changed every other day until they reached confluence, 6–9 days after plating.

The conditionally immortalized proximal tubular epithelial cells (IM-PTEC) were generated as previously described (Stokman *et al.*, 2011). Cells were grown in HK-2 medium [DMEM/F12 medium with 10% FBS, 5 $\mu g \cdot mL^{-1}$ insulin and transferrin, 5 $ng \cdot mL^{-1}$ sodium selenite, 20 $ng \cdot mL^{-1}$ tri-iodothyrionine, 50 $ng \cdot mL^{-1}$ hydrocortisone, 5 $ng \cdot mL^{-1}$ prostaglandin E_1, with L-glutamine, antibiotics and mouse IFN-γ

(1 ng·mL^{-1}, R&D Systems, Minneapolis, MN, USA)] at 33°C in 5% CO_2 and 95% air. For experiments, cells were cultured under restrictive conditions at 37°C in the absence of IFN-γ for 7 days.

The human breast cancer cell lines MCF7, HBL100, BT474, BT549, T47D and MDA-MB-231 were cultured as described (de Graauw *et al.*, 2010). The human lung cancer cell lines H460, A549 and H1299 were obtained from American Type Culture Collection (ATCC, Manassas, VA) and cultured in RPMI 1640 Medium (Invitrogen) supplemented with 10% FBS. The human clear cell renal cell carcinoma cell line RCC10 was kindly provided by Dr Rachel Giles (UMC Utrecht, the Netherlands) and was cultured in DMEM (Invitrogen) supplemented with 10% FBS.

siRNA transfection and treatments

Thermo Scientific Dharmacon siGENOME SMARTpools, targeting mouse RAPGEF3/EPAC1 (M-057800–00), RAP1A (M-057058–01) and RAP1B (M-062638–01) were purchased from Thermo Fischer Scientific (Lafayette, CO). The siRNA targeting green fluorescent protein (siGFP) was used as a control siRNA. For siRNA reverse transfection, cell suspension was transfected with siRNA at a final concentration of 100 nM (50 nM each for siRNAs targeting RAP1A and RAP1B) using INTERFERin™ siRNA transfection reagent (PolyPlus-transfection, Illkirch, France) according to the manufacturer's instruction. Cells were kept for 48–72 h before experiments, and the efficiency of siRNAs was evaluated by Western blotting using specific antibodies against Epac1 and Rap1.

Primary mouse renal cells cultured in 96-well plates or 6-well plates were treated in complete culture medium with indicated concentrations of cisplatin in the presence or absence of 100 μM 8-pCPT-2′-O-Me-cAMP or 10 μM forskolin. After the indicated times, cell morphology was microscopically examined, and apoptosis was determined by cell cycle analysis and caspase-3 activity assay, as well as the level of cleaved caspase-3.

Confluent monolayers of IM-PTEC in 96-well plates, 24-well plates containing glass coverslips or 6-well plates were exposed to 25 μM cisplatin, 100 μM 8-pCPT-2′-O-Me-cAMP or both. In some experiments, cells were exposed to 10 μM N6-Bnz-cAMP-AM or isoproterenol in the presence or absence of 25 μM cisplatin. To monitor cell–cell contacts by immunofluorescence, cells were fixed after 16 h. After 24 h, cell apoptosis was determined by cell cycle analysis or caspase-3 activity assay.

Confluent cancer cells in 96-well plates were exposed to cisplatin (0–100 μM), in the presence or absence of 100 μM 8-pCPT-2′-O-Me-cAMP. Cell apoptosis was determined using caspase-3 activity assay after 24 and 48 h.

Rap1-GTP pulldown assay

Rap1 activation was assayed as previously described (Stokman *et al.*, 2011). Briefly, cells were starved in serum-free medium for 1 h and then incubated with different analogues for 15 min, except for isoprenaline where cells were treated for 5 min. In some experiments, IM-PTEC cells were treated with 25 μM cisplatin, in the presence or absence of 100 μM 8-pCPT-2′-O-Me-cAMP, for 6 h in HK-2 medium. After the incubation, cells were washed with cold PBS containing 1 mM $MgCl_2$ and lysed on ice for 15 min with lysis buffer containing 10% (v/v) glycerol, 1% (v/v) Nonidet P-40, 50 mM Tris–HCl, pH 7.4, 200 mM NaCl, 2.5 mM $MgCl_2$ supplemented with 1 μM aprotonin and 2 μM leupeptide. Lysates were centrifuged, and active Rap in the supernatant was precipitated with glutathione Sepharose 4B beads (GE Healthcare, Buckinghamshire, UK) pre-coated with a GST fusion protein of RalGDS-RBD. Both precipitate and supernatant were subjected to Western blotting to detect GTP-bound Rap1 and total Rap1 respectively.

Western blotting

Cells were washed twice with ice-cold PBS and harvested in lysis buffer as above supplemented with protease inhibitor cocktail II (Sigma). The protein concentration was determined using BCA protein assay (Thermo Fisher Scientific, Rockford, IL, USA) with BSA as a standard. Equal amounts of protein were separated by SDS-PAGE and transferred to Immobilon-P (Millipore, Amsterdam, the Netherlands). Membranes were blocked in 5% (w/v) BSA in Tris-buffered saline/Tween 20 (TBS-T, 0.5 M NaCl, 20 mM Tris–HCl and 0.05% (v/v) Tween 20, pH 7.4) for 1 h at room temperature. The incubation of primary antibodies against Rap1, Epac1, pSer^{133}-CREB, tubulin, cleaved caspase-3 was performed overnight at 4°C. Thereafter, blots were incubated with HRP or Cy5-conjugated secondary antibody in 1% BSA in TBS-T for 1 h at room temperature. Protein signals were detected with ECL Plus reagent (GE Healthcare) by imaging with the Typhoon 9400 (GE Healthcare).

Caspase-3 activity assay

For exposures performed in six-well plates, both attached and detached cells were collected and centrifuged (900× *g*, 5 min, 4°C). The cell pellet was re-suspended in lysis buffer (10 mM HEPES, 40 mM β-glycerophosphate, 50 mM NaCl, 2 mM $MgCl_2$ and 5 mM EGTA) and subjected to three cycles of freezing in liquid nitrogen and thawing to fracture cells. The suspension was centrifuged at 17 000× *g* for 30 min, and the supernatant, containing cytoplasmic fraction, was collected. The protein concentration was determined by Bradford protein assay (Bio-Rad Laboratories, Munich, Germany) using IgG as a standard. Equal amounts of protein (10 μg) were used for measuring caspase-3 activity with Ac-DEVD-AMC as the substrate (25 μM). AMC fluorescence was followed in time using a fluorescence plate reader (FLUOstar OPTIMA, BMG LABTECH, Offenburg, Germany). Caspase-3 activity was calculated as pmol min^{-1} mg^{-1} using AMC as a standard.

For the exposure in 96-well microplates (Greiner Bio-One), five times concentrated lysis buffer (250 mM HEPES, pH 7.4, 25 mM CHAPS, 25 mM DTT) was added after exposure, and cells were lysed on ice for 30 min. The protein concentration was determined by BCA protein assay using BSA as a standard. The caspase-3 activity was measured as above. In some experiments, caspase-3 activity was normalized to cisplatin alone group (as 100%).

Cell cycle analysis

After the exposure, both attached and detached cells were collected, centrifuged (900× *g*, 10 min, 4°C) and then re-suspended in 90% ethanol for fixation (–20°C). Fixed cells

were centrifuged and washed once with PBS followed by re-suspension in PBS–EDTA containing 7.5 μM propidium iodide and 10 μg·mL^{-1} RNase A. After 30 min at room temperature, cells were analysed by flow cytometry (FACSCalibur; BD Biosciences, Franklin Lakes, NJ). The amount of cells in sub-G_0/G_1, indicating the percentage of apoptotic cells, was calculated using the CellQuest software (BD Biosciences).

Real-time quantitative PCR (Q-PCR)

Total RNA was isolated from cells using an RNeasy Plus Mini Kit (Qiagen, Hilden, Germany) according to the manufacturer's protocol. RNA was reverse transcribed for cDNA with RevertAid H Minus First strand cDNA Synthesis Kit (Thermo Fisher Scientific).

Real-time Q-PCR for Epac1 mRNA expression was performed on the ABI PRISM 7700 Sequence Detector by using the SYBR Green PCR Master Mix Kit (Applied Biosystems, Foster City, CA USA). Hypoxanthine phophoribosyltransferase gene (HPRT, forward 5′-ATGGGAGGCCATCACATTGT-3′; reverse 5′-ATGTAATCCAGCAGGTCAGCAA-3′) was found to be equally expressed in all the tested cell lines, thus was used as internal standard. Human Epac1 primers (forward: 5′-CTGCTGAGGGAGCAGTGG-3′; reverse: 5′-AGCCAAACAG GCAAGTTCC-3′) were designed by online ProbeFinder software (Roche Applied Science) and purchased from Eurogentec (Maastricht, the Netherlands). The cycling condition was as follows: initial denaturation at 95°C for 10 min, followed by 40 cycles consisting of denaturation at 95°C for 15 s and amplification at 60°C for 1 min. The average C_T value was calculated from triplicates of each sample. The relative Epac1 mRNA expression in each cell line was calculated using the $2^{-\Delta\Delta CT}$ method (Livak and Schmittgen, 2001) and expressed as fold change of normalized Epac1 expression level in RCC10.

Immunofluorescence and imaging techniques

Cells were cultured on glass coverslips in 24-well plates. After exposure, cells were fixed with 3.7% formaldehyde for 20 min and permeabilized with 0.4% (w/v) Triton X-100 in PBS for 10 min, followed by three washes with PBS. After blocking with 5% (v/v) normal goat serum (Vector Laboratories, Burlingame, CA, USA) and 1% (w/v) BSA in PBS, cells were stained for anti-β-catenin and anti-ZO-1 overnight at 4°C. Thereafter, cells were washed three times with PBS and subsequently incubated with Alexa 488 or Cy3-labelled secondary antibodies, in combination with 2 μg·mL^{-1} Hoechst 33258 (1 h at room temperature). Coverslips were mounted on glass slides using Aqua-Poly/Mount (Polysciences, Warrington, PA) and imaged using a Nikon E600 epifluorescence microscope (Nikon, Tokyo, Japan) with a 60× Plan Apo NA1.4 objective lens (Nikon).

Quantitative analysis of cell–cell junctions

To segment the β-catenin and ZO-1 image signals, we adapted the watershed masked clustering algorithm, whereby the cell periphery is predicted to be equidistant from adjacent nuclei. This prediction was anchored by fluorescence signal that was present in this area, which was also extrapolated to generate an intact line using a watershed algorithm. As an indicator of cell–cell junction strength, the average area occupied by β-catenin fluorescence signal in the cell–cell junction region of each cell was calculated and expressed as area per nucleus in pixels. To quantify the ZO-1 signal at cell–cell junctions, we measured the percentage of the cell border that was positive for ZO-1 staining at the periphery of each cell ('intactness'). To do this, the ZO-1 fluorescence was overlaid with the predicted intact line (described above). A continuous line encircling a cell was given a score of 100%, while interrupted staining scored proportionately lower values. This 'intactness' parameter was considered most appropriate in view of the function of ZO-1 and tight junctions to provide a continuous seal around each cell at the apical membrane. The analysis was performed using ImageJ 1.44i software.

Statistical procedures

Data are expressed as mean ± SEM. Data from cell–cell junction quantification were analyzed using the non-parametric Kolmogorov–Smirnow (KS) test. All the other data were tested for normality and passed the KS test ($\alpha = 0.05$). Statistical significance was determined using an unpaired *t*-test. Values of $P \leq 0.05$ were considered statistically significant. All statistical analyses were performed using GraphPad Prism 4 (GraphPad Software, San Diego, CA).

Materials

Mouse monoclonal antibody to Epac1 (5D3, available from Cell Signaling, Danvers, MA) was generated in the laboratory of J L Bos, Utrecht, the Netherlands. The primary antibodies used were as follows: rabbit-anti-Rap1 from Santa Cruz Biotechnology Inc. (Santa Cruz, CA); rabbit-anti-phospho-CREB (Ser^{133}) from Cell Signaling); rabbit-anti-cleaved caspase-3 from Upstate Biotechnology (Lake Placid, NY); mouse-anti-vinculin and anti-tubulin from Sigma-Aldrich (St. Louis, MO); mouse anti-β-catenin from BD Biosciences (San Jose, CA) and rabbit-anti-zona occludens-1 (ZO-1) from Zymed (Burlington, NC). The secondary antibodies conjugated to horseradish peroxidase (HRP) and Cy5 were purchased from Jackson Immunoresearch (Newmarket, UK); antibodies coupled to Alexa-488 and Cy3, as well as rhodamine phalloidin, were from Invitrogen (Breda, the Netherlands).

8-pCPT-2′-O-Me-cAMP, 8-pCPT-2′-O-Me-cAMP-AM and N6-Bnz-cAMP-AM were from BIOLOG Life Sciences (Bremen, Germany). Forskolin was purchased from Calbiochem (Nottingham, UK). Acetyl-Asp-Glu-Val-Asp-AMC (Ac-DEVD-AMC) was obtained from Enzo Life Sciences (Zandhoven, Belgium). *Cis*-diammineplatinum(II) dichloride (cisplatin), collagenase (Crude: Type XI), isoprenaline, propidium iodide, RNase A, 7-amino-4-methylcoumarin (AMC) and other reagents not specifically mentioned were obtained from Sigma-Aldrich.

Results

cAMP signalling protects against cisplatin-induced apoptosis in primary mouse renal cells

To determine cisplatin-induced apoptotic cell death, confluent primary mouse renal cells were treated with cisplatin in a dose- and time-dependent manner, and caspase-3 activity was measured. Treatment with cisplatin led to an induction of apoptosis, starting at 18 h after 25–75 μM of cisplatin treat-

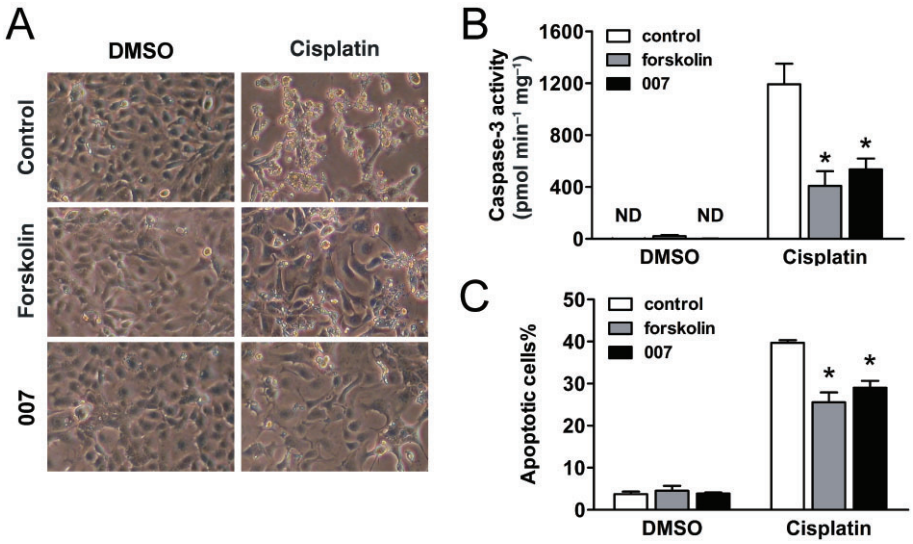

Figure 1

Activation of cAMP signalling protects primary mouse renal cells against cisplatin-induced apoptosis. Primary mouse renal cells were exposed to 25 μM cisplatin for 24 h, in the presence or absence of 10 μM forskolin or 100 μM 8-pCPT-2′-O-Me-cAMP (007). (A) Cell morphology was monitored by light microscopy, and representative images are shown. Original magnification: 10×. Apoptosis was determined by (B) caspase-3 activity assay and (C) cell cycle analysis. Data are expressed as mean ± SEM of three independent experiments ($n = 3$). *$P < 0.05$, significantly different from cisplatin alone. ND indicates that value is not detectable.

ment (Supplementary data, Figure S1A). This effect was confirmed by measurement of caspase-3 activation by Western blotting, which revealed pronounced cleavage of caspase-3 that was detectable at 24 h exposure with 25 μM cisplatin (Supplementary data, Figure S1B).

To investigate the effect of cAMP signalling on cisplatin-induced apoptosis in primary mouse renal cells, confluent monolayers were exposed to 25 μM cisplatin, in the presence or absence of 10 μM forskolin or 100 μM 8-pCPT-2′-O-Me-cAMP. Forskolin induces cAMP synthesis via adenylate cyclase activation and therefore activates all downstream effectors, including PKA and Epac, whilst 8-pCPT-2′-O-Me-cAMP is an Epac-selective cAMP analogue that preferentially activates Epac (Enserink *et al.*, 2002). Microscopic examination after a 24 h exposure showed that cisplatin treatment resulted in disruption of cell–cell interactions and induced massive cell detachment, which was profoundly reduced by simultaneous treatment with either forskolin or 8-pCPT-2′-O-Me-cAMP (Figure 1A). Cisplatin-induced cell detachment coincided with increased caspase-3 activity and a higher percentage of cells with hypodiploid DNA content (i.e. sub-G_0/G_1), confirming that cisplatin induced apoptosis in these cells. Activation of Epac–Rap signalling by either forskolin or 8-pCPT-2′-O-Me-cAMP significantly inhibited cisplatin-induced caspase-3 activation and reduced the percentage of cells in sub-G_0/G_1 phase of the cell cycle, indicating a protective effect on these cells against cisplatin-induced apoptosis (Figure 1B and C). The similar degree of protection by forskolin and 8-pCPT-2′-O-Me-cAMP suggests that cAMP signalling confers protection predominantly via activation of Epac in these cells.

Taken together, these data indicate that Epac signalling can be activated by cAMP to protect against cisplatin-induced apoptosis in primary mouse renal cells.

8-pCPT-2′-O-Me-cAMP activates Epac–Rap signalling and protects against cisplatin-induced apoptosis in IM-PTEC

In the kidney, the proximal tubules are the principal sites of cisplatin-induced nephrotoxicity (Townsend *et al.*, 2003; Vickers *et al.*, 2004) and also show high Epac1 expression (Honegger *et al.*, 2006). Therefore, we used IM-PTEC, a conditionally SV40-immortalized mouse proximal tubular epithelial cell line for further study (Stokman *et al.*, 2011). First, to determine whether Epac–Rap signalling is functional in IM-PTEC, we determined whether Epac1 protein was expressed and the ability of cAMP to activate Epac–Rap1 signalling. Epac activation is associated with a conformational change allowing the binding and activation of Rap (Rehmann *et al.*, 2006; 2008); thus, the activation of Epac is measured indirectly through measurement of activation of the Epac target, Rap1 using a Rap1-GTP pulldown (activity) assay. As shown in Figure 2A, IM-PTEC cells expressed endogenous Epac1. More importantly, the Epac-selective cAMP analogues 8-pCPT-2′-O-Me-cAMP and its highly membrane-permeable ester form 8-pCPT-2′-O-Me-cAMP-AM, and also the adenylate cyclase activator forskolin increased Rap1 activation, indicating that Epac–Rap signalling is induced by cAMP in these cells (Figure 2A and B). Similarly, Epac–Rap signalling was also observed in primary mouse renal cells (Supplementary data, Figure S2).

Second, IM-PTEC cells were exposed to 25 μM cisplatin, 100 μM 8-pCPT-2′-O-Me-cAMP or both to determine the effect of Epac–Rap activation on cisplatin-induced apoptosis. Rap1 activation was determined after 6 h of treatment. Rap1 activation by 8-pCPT-2′-O-Me-cAMP was similar in both DMSO- and cisplatin-treated cells, showing that cisplatin

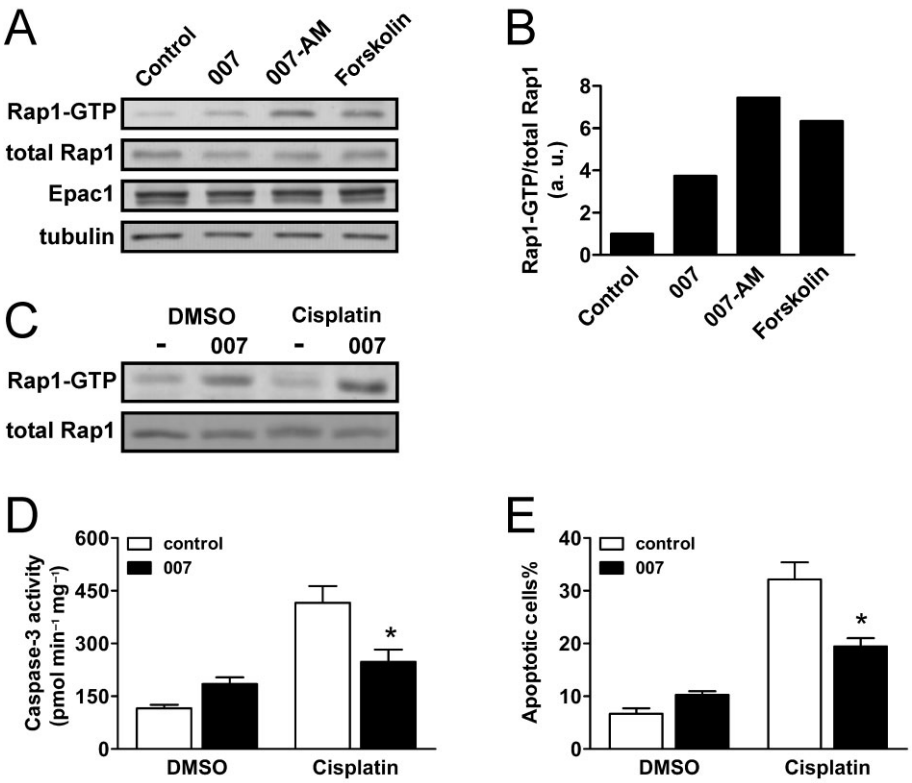

Figure 2

8-pCPT-2′-O-Me-cAMP activates Epac–Rap signalling and protects IM-PTEC against cisplatin-induced apoptosis. (A) IM-PTEC were exposed to vehicle (10 mM Tris–HCl, pH 7.4, 50 mM NaCl) as control, 100 μM 8-pCPT-2′-O-Me-cAMP (007), 2.5 μM 8-pCPT-2′-O-Me-cAMP-AM (007-AM) or 10 μM forskolin for 15 min. Lysates were used for detection of active GTP-bound Rap1 levels by pulldown analysis followed by immunoblotting. The expression of total Rap1 and Epac1 was confirmed by Western blotting. Blots shown are representative of four independent experiments. (B) Densitometric analysis of the blots in (A) determined the ratio of Rap1-GTP/total Rap1 and normalized to control. (C) IM-PTEC were exposed to vehicle or 100 μM 8-pCPT-2′-O-Me-cAMP (007), in the presence or absence of 25 μM cisplatin in complete HK2 medium for 6 h. The active GTP-bound and total Rap1 levels were detected by pulldown analysis followed by immunoblotting. Blots shown are representative of three independent experiments. (D–E) IM-PTEC were exposed to 25 μM cisplatin for 24 h, in the presence or absence of 100 μM 8-pCPT-2′-O-Me-cAMP (007). Apoptosis was determined by (D) caspase-3 activity assay and (E) cell cycle analysis. Data are expressed as mean ± SEM of three independent experiments ($n = 3$). *$P < 0.05$, significantly different from cisplatin alone.

does not disrupt 8-pCPT-2′-O-Me-cAMP activation of Epac–Rap signalling (Figure 2C). After 24 h, cell apoptosis was determined by caspase-3 activity and cell cycle analysis. Although IM-PTEC cells were somewhat more resistant to cisplatin compared with primary cells and did not show significant cell detachment, 8-pCPT-2′-O-Me-cAMP still showed a protective effect against apoptosis (Figure 2D and E).

Taken together, these results are consistent with those observed in the heterogeneous mix of primary mouse renal cells and demonstrate that Epac–Rap signalling functions to specifically protect proximal tubular epithelial cells against cisplatin-induced apoptosis.

The protective effect of 8-pCPT-2′-O-Me-cAMP against cisplatin-induced apoptosis is Epac–Rap dependent

Although 8-pCPT-2′-O-Me-cAMP is an Epac-selective activator, to confirm that Epac–Rap signalling confers the observed antiapoptotic effects, we disrupted Epac–Rap signalling in IM-PTEC by silencing Epac1 and Rap1 gene expression. Transfection of IM-PTEC cells with siRNAs targeting against Epac1 and Rap1 resulted in significant reduction in Epac1 and Rap1 expression respectively (Figure 3A and B). As expected, the knockdown of Epac1 (or Rap1) prevented 8-pCPT-2′-O-Me-cAMP induction of Rap1 activation in these cells, whilst 8-pCPT-2′-O-Me-cAMP was still able to activate Rap1 in control siGFP-transfected cells (Figure 3A). In both untransfected and siGFP-transfected cells, the co-incubation of 8-pCPT-2′-O-Me-cAMP significantly reduced the high percentage of apoptotic cells caused by cisplatin treatment (Figure 3C). However, the ability of 8-pCPT-2′-O-Me-cAMP to inhibit cell apoptosis was impaired in either Epac1 or Rap1 knockdown cells, concordant with the suppression of Rap1 activation in these knockdown cells. These results demonstrate that Epac–Rap signalling is required for 8-pCPT-2′-O-Me-cAMP-mediated protection against cisplatin-induced apoptosis.

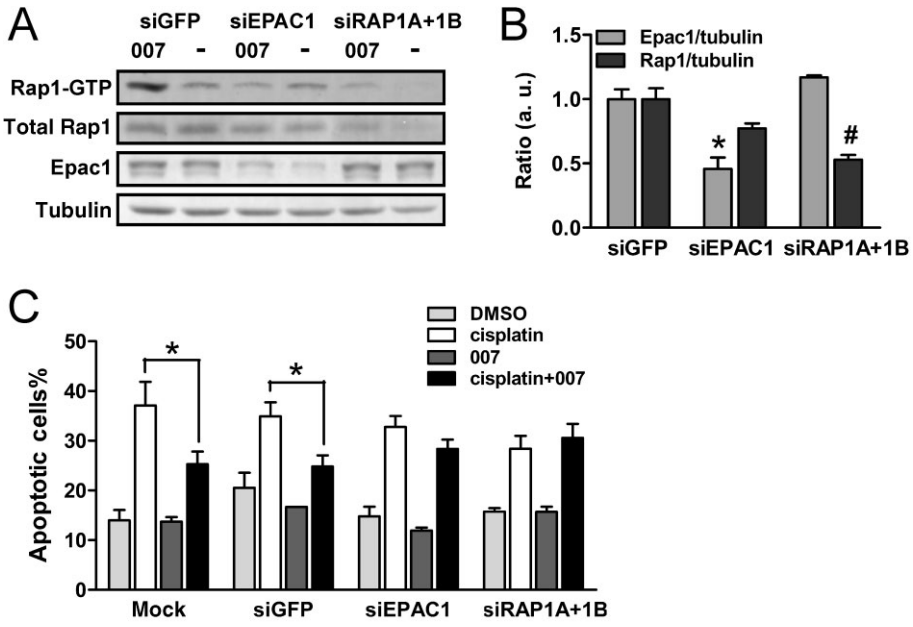

Figure 3

8-pCPT-2′-O-Me-cAMP-mediated antiapoptotic effect is Epac–Rap dependent. (A) The active GTP-bound Rap1 level after 15 min incubation in the presence or absence of 100 μM 8-pCPT-2′-O-Me-cAMP (007), as well as the expression of Epac1 and Rap1 were detected as above in siRNA-transfected IM-PTEC. The siGFP was used as a control siRNA. Blots shown are representative of three independent experiments. (B) Densitometric analysis of the blots in (A) determined the ratio of Epac1/tubulin and Rap1/tubulin and normalized to siGFP-transfected IM-PTEC. Data are expressed as mean ± SEM of duplicates for each siRNA ($n = 2$). *$P < 0.05$, significant difference between siEPAC1- and siGFP-transfected cells. #$P < 0.05$, significant difference between siRAP1A + 1B- and siGFP-transfected cells. (C) Mock- or siRNA-transfected IM-PTEC were exposed to 25 μM cisplatin for 24 h, in the presence or absence of 100 μM 8-pCPT-2′-O-Me-cAMP (007). Apoptosis was determined by cell cycle analysis. Data are expressed as mean ± SEM of three independent experiments ($n = 3$). *$P < 0.05$, significant difference between two groups.

Endogenous cAMP protects IM-PTEC against cisplatin-induced apoptosis via Epac–Rap signalling

The β-adrenoceptor increases intracellular cAMP levels via Gs coupling to adenylate cyclase. Both Epac and PKA have been found to participate in a wide range of β-adrenoceptor -mediated biological processes, including integrin-mediated cell adhesion and gap junction formation (Rangarajan *et al.*, 2003; Somekawa *et al.*, 2005). As the β-adrenoceptor is also expressed in the kidney, we examined whether this cAMP-elevating GPCR reproduces the antiapoptotic effect of 8-pCPT-2′-O-Me-cAMP in IM-PTEC.

Stimulation with isoprenaline, a ligand for the β-adrenoceptor, induced both activation of Rap1 and phosphorylation of the cAMP response element binding protein (CREB) (Figure 4A and B), indicating that both Epac and PKA pathways were activated. In contrast, the PKA-selective analogue N6-Bnz-cAMP-AM induced phosphorylation of CREB but not Rap1 activation, whereas the Epac-selective analogues 8-pCPT-2′-O-Me-cAMP and 8-pCPT-2′-O-Me-cAMP-AM activated Rap1 but not CREB. The adenylate cyclase activator forskolin also induced both Rap1 activation and phosphorylation of CREB (Figure 4A and B). We then looked at the effect of these compounds on cisplatin-induced apoptosis in IM-PTEC. Treatment with isoprenaline significantly decreased cisplatin-induced elevation of caspase-3 activity, similar to that observed with 8-pCPT-2′-O-Me-cAMP treatment (Figure 4C). However, N6-Bnz-cAMP-AM did not blunt cisplatin-induced apoptosis, suggesting that the anti-apoptotic effect of cAMP signalling was not induced by PKA activation. More importantly, the protective effect of isoprenaline against cisplatin-induced elevation of caspase-3 activity was blocked in both Epac1 and Rap1 knockdown cells, confirming a critical involvement of Epac1–Rap1 in the protection (Figure 4D).

These results demonstrate that endogenous cAMP signalling induced by cell surface receptors can protect IM-PTEC from cisplatin-induced apoptosis, and that this protection is dependent on Epac–Rap signalling.

8-pCPT-2′-O-Me-cAMP stabilizes cell–cell junctions and protects against cisplatin-induced disruption of cell–cell adhesions in IM-PTEC

The small GTPase Rap is regarded as an important regulator of cell–cell and cell–matrix adhesions. These adhesions provide direct cellular survival signals and also structural elements required for essential cellular functions, such as cell polarity. We explored the hypothesis that Epac activation also contributed to the stabilization of cell adhesions in IM-PTEC. As cisplatin treatment did not result in significant loss of cell–matrix adhesion in IM-PTEC, we determined the effect of active Epac–Rap signalling on two major types of cell–cell adhesions, adherens junctions and tight junctions. Immunofluorescence staining showed that β-catenin and ZO-1 were predominantly localized at the cell membrane as expected

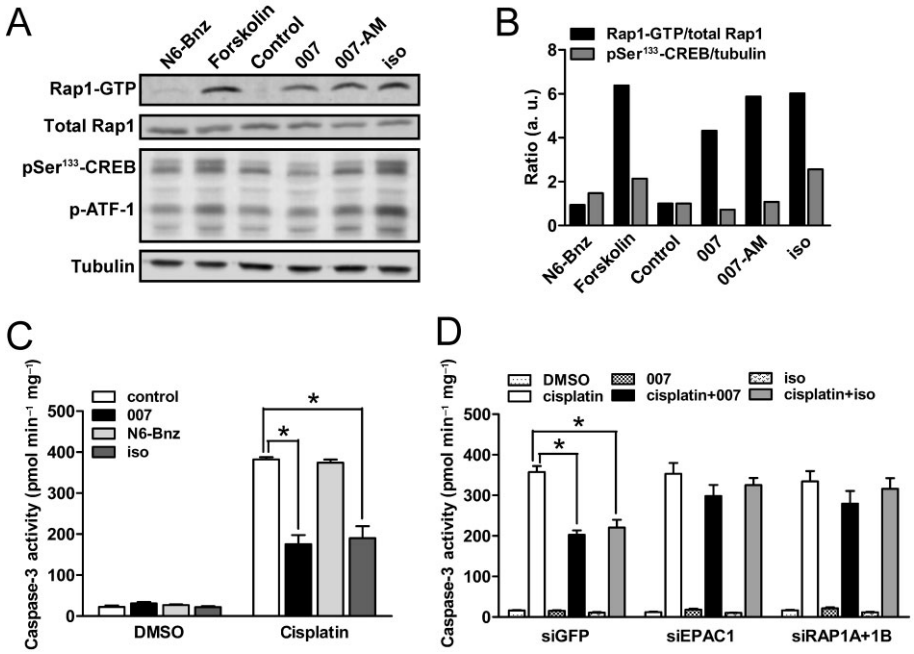

Figure 4

cAMP protects IM-PTEC against cisplatin-induced apoptosis via Epac–Rap signalling. (A) IM-PTEC were exposed to vehicle as control, 100 μM 8-pCPT-2′-O-Me-cAMP (007), 2.5 μM 8-pCPT-2′-O-Me-cAMP-AM (007-AM), 10 μM forskolin, 10 μM PKA-selective analogue N6-Bnz-cAMP-AM (N6-Bnz) for 15 min, or 10 μM β-adrenoceptor agonist isoprenaline (iso) for 5 min. Lysates were used for detection of active GTP-bound Rap1 levels by pulldown analysis followed by immunoblotting. The expression of total Rap1 and phosphorylation of CREB at Ser^{133} was confirmed by Western blotting. Blots shown are representative of three independent experiments. (B) Densitometric analysis of the blots in (A) determined the ratio of Rap1-GTP/total Rap1 and $pSer^{133}$-CREB/tubulin and normalized to control. (C) IM-PTEC were exposed to 25 μM cisplatin for 24 h, in the presence or absence of 100 μM 8-pCPT-2′-O-Me-cAMP (007), 10 μM N6-Bnz-cAMP-AM (N6-Bnz) or 10 μM isoprenaline (iso). Apoptosis was determined by caspase-3 activity assay. Data are expressed as mean ± SEM of three independent experiments (n = 3). *P < 0.05, significant difference between two groups. (D) siRNA-transfected IM-PTEC were exposed to 25 μM cisplatin for 24 h, in the presence or absence of 100 μM 8-pCPT-2′-O-Me-cAMP (007) or 10 μM iso. Apoptosis was determined by caspase-3 activity assay. Data are expressed as mean ± SEM of three independent experiments (n = 3). *P < 0.05, significant difference between two groups.

(Figure 5A). We measured the fluorescence signal from these proteins at cell–cell junctions using quantitative digital image analysis (Figure 5B and C). For β-catenin, a component of adherens junctions that confers strength to the cell–cell interaction, we measured the total amount of staining in the junction area per cell. For ZO-1, a component of tight junctions at the apical membrane that provides a water-tight seal to the epithelial layer, we measured the degree of intactness of the junction staining (percentage intact junction around each cell). Figure 5A-C show that cisplatin treatment caused loss of both proteins from the plasma membrane, indicating a reduction in cell–cell adhesions. The treatment with 8-pCPT-2′-O-Me-cAMP strongly reduced the loss of β-catenin and ZO-1 caused by cisplatin, indicating a protective effect against cell–cell junction disruption.

These results demonstrate that Epac–Rap activation by 8-pCPT-2′-O-Me-cAMP enhances cell–cell adhesions in IM-PTEC and protects cells from cisplatin-induced disruption of both adherens junctions and tight junctions.

8-pCPT-2′-O-Me-cAMP protects IM-PTEC against cisplatin-induced disruption of cell–cell adhesions via Epac–Rap activation

To confirm that 8-pCPT-2′-O-Me-cAMP-mediated protection of cell–cell junctions was also dependent on Epac–Rap signalling, Epac1 and Rap1 knockdown cells were exposed to either cisplatin alone or in combination with 8-pCPT-2′-O-Me-cAMP and then immunostained for β-catenin and ZO-1. The fluorescence signal from both proteins at cell–cell junctions was measured using quantitative digital image analysis as above. As shown in Figure 6, most of both fluorescence signals disappeared from cell–cell contacts after treatment with cisplatin in untransfected and siRNA-transfected cells. Simultaneous treatment with 8-pCPT-2′-O-Me-cAMP rescued both the loss of β-catenin at the junction area and the loss of ZO-1 at the plasma membrane in either untransfected or siGFP-transfected cells. However, the preservation of either β-catenin or ZO-1 by 8-pCPT-2′-O-Me-cAMP against cisplatin was inhibited in both Epac1 and Rap1 knockdown cells, indicating that Epac–Rap signalling is required for 8-pCPT-2′-O-Me-cAMP-mediated stabilization of adherens and tight junctions. These results suggest that the activation of Epac–Rap signalling stabilizes cell–cell adhesions and protects them from cisplatin-induced disruption.

8-pCPT-2′-O-Me-cAMP does not protect Epac-deficient cancer cells from cisplatin-induced cell killing

Whilst 8-pCPT-2′-O-Me-cAMP protects renal cells during cisplatin treatment, it should not compromise the capacity of

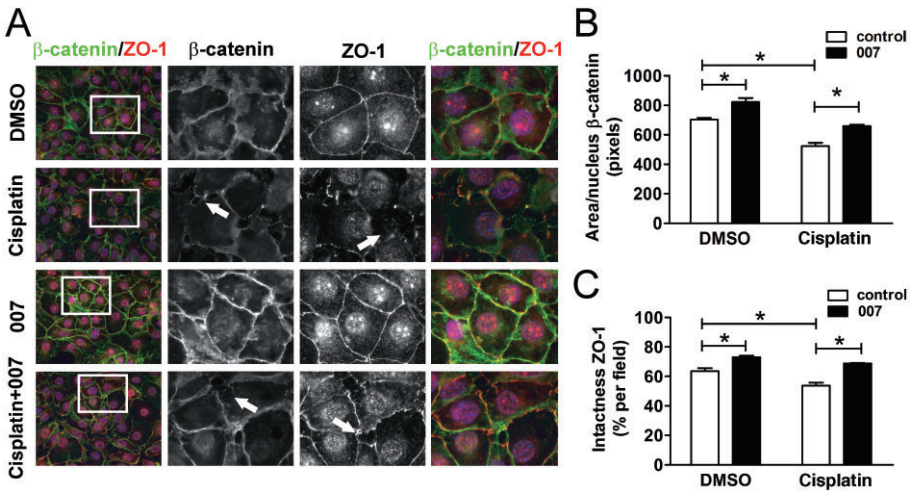

Figure 5

8-pCPT-2′-O-Me-cAMP stabilizes cell–cell junctions and protects IM-PTEC from cisplatin-induced cell junction disruption. (A) IM-PTEC were exposed to 25 μM cisplatin for 16 h, in the presence or absence of 100 μM 8-pCPT-2′-O-Me-cAMP (007). Cells were fixed and stained for β-catenin (green) and ZO-1 (red). Images shown are representative of three independent experiments. Original magnification: 60×. Arrows show gaps between cells, indicating disruption of monolayer integrity by cisplatin. (B) The area of β-catenin fluorescence at the cell junctions was quantified, and the average area occupied by β-catenin in each cell was calculated and expressed as area per nucleus in pixels. (C) The ZO-1 fluorescence at the cell junctions was identified. The percentage of the cell border that overlapped with ZO-1 localization was calculated and expressed as intactness ZO-1 per field. Data are representative of three independent experiments and expressed as mean ± SEM ($n = 3$). *$P < 0.05$, significant difference between two groups.

cisplatin to kill tumour cells. We therefore examined the effect of 8-pCPT-2′-O-Me-cAMP on cisplatin-induced tumour cell killing using a panel of human cancer cell lines. Since cisplatin has been applied in the chemotherapy of lung and breast cancers, we tested human lung cancer cell lines H460, A549 and H1299, as well as human breast cancer cell lines MCF7, HBL100, BT474, BT549, T47D and MDA-MB-231.

All the cancer cell lines were exposed to a range of cisplatin concentrations. Four cell lines H460, A549, HBL100 and BT549 showed significant cell apoptosis, whereas the others were resistant to cisplatin treatment (data not shown). Therefore, the EC_{50} of each cell line for cisplatin-induced cell apoptosis was determined by caspase-3 activity assay (supplementary data, Table S1), and these four cell lines were used for further exposure experiments.

The Epac1 protein level was determined by Western blotting in all tested human cancer cell lines. Two out of three lung cancer cell lines and five out of six breast cancer cell lines had undetectable Epac expression (data not shown), which is consistent with the low mRNA level of RAPGEF3/EPAC1 in most of NCI60 cancer cell lines tested in a HG-U133A array (data available at GNF BioGPS http://biogps.gnf.org/#goto=genereport&id=10411). Among the four selected cancer cell lines, H460 was the only one that exhibited detectable Epac1 protein, which was low compared with kidney epithelial cells (Figure 7A and B). The Epac1 mRNA level was determined by real-time Q-PCR in these four cancer cell lines, with RCC10, a renal cell carcinoma cell line that expresses considerable Epac1, as positive control. Again, H460 was the only cell line that expressed Epac1 mRNA, which was consistent with the pattern at protein level (Figure 7A and D).

We next tested the effect of 8-pCPT-2′-O-Me-cAMP on cisplatin-induced cancer cell apoptosis in the selected cell lines. The concentration of cisplatin for each cell line was chosen according to the EC_{50} dose. Cells were exposed to cisplatin for 24 h, in the presence or absence of 8-pCPT-2′-O-Me-cAMP, and cell apoptosis was determined using a caspase-3 activity assay. Both primary mouse renal cells and IM-PTEC were included as controls. As shown in Figure 7C, 8-pCPT-2′-O-Me-cAMP significantly inhibited the elevated caspase-3 activity in H460 cells, as it did in primary mouse renal cells and IM-PTEC, whereas there was no protection against apoptosis in Epac-deficient A549, HBL100 and BT549 cells.

These results suggest that while Epac activation reduces cisplatin-mediated damage to kidney epithelial cells, it does not reduce the chemotherapeutic effect towards cancer cells in which Epac expression is absent.

Discussion and conclusions

Our results demonstrate that cAMP signalling protects mouse proximal tubular epithelial cells against cisplatin-induced cytotoxicity via activation of the Epac–Rap signalling pathway. First, cAMP-mediated protection from cytotoxicity was independent of PKA but dependent on Epac activation, as the protection could be induced with the Epac-selective activator 8-pCPT-2′-O-Me-cAMP and was prevented by siRNA-mediated depletion of Epac1 and Rap1 proteins. Furthermore, a PKA-selective cAMP analogue was not able to induce protection against apoptosis. This identifies Epac–Rap signalling as a cAMP-dependent cytoprotective pathway.

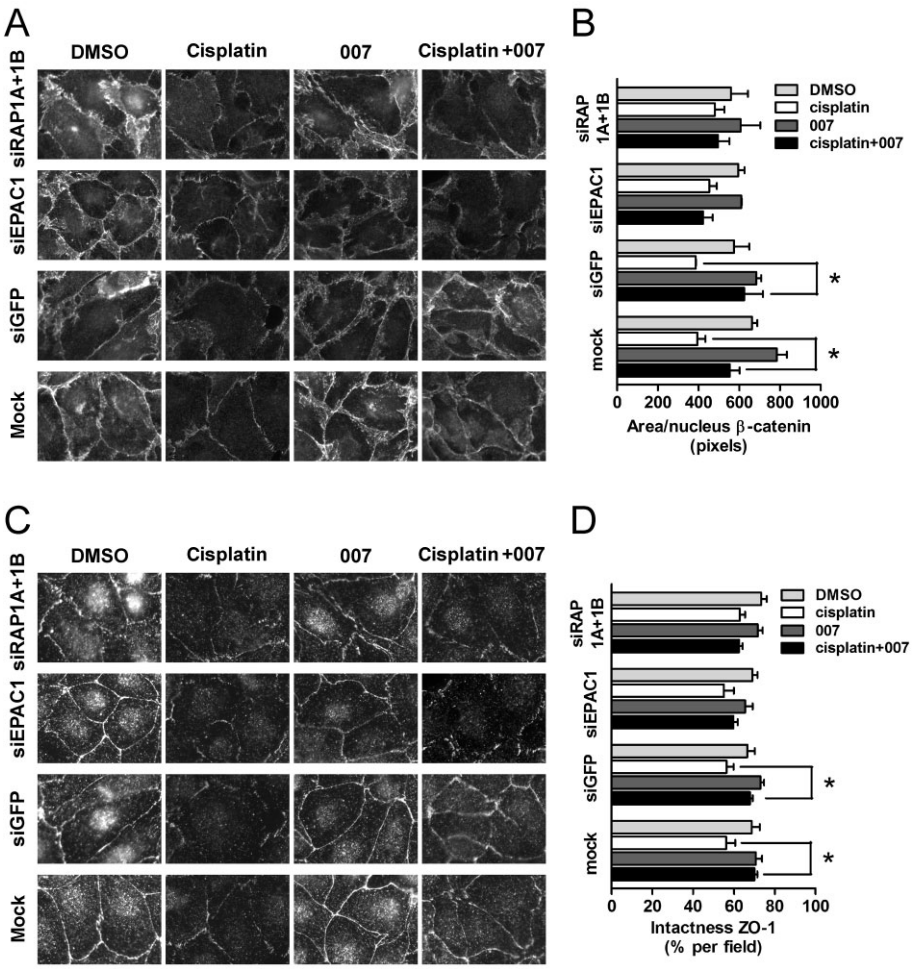

Figure 6

8-pCPT-2′-O-Me-cAMP-mediated cell junction preservation is Epac–Rap dependent. Mock- or siRNA-transfected IM-PTEC were exposed to 25 μM cisplatin, in the presence or absence of 100 μM 8-pCPT-2′-O-Me-cAMP (007). After 16 h, cells were fixed and stained for (A) β-catenin and (C) ZO-1. Images shown are representative of three independent experiments. Original magnification: 60×. (B) Average area occupied by β-catenin in each cell was calculated and expressed as area per nucleus in pixels. (D) The percentage of the cell border that overlapped with ZO-1 localization was calculated and expressed as intactness ZO-1 per field. Data are representative of three independent experiments and expressed as mean ± SEM (n = 3). *P < 0.05, significant difference between two groups.

Second, Epac activation prevented disruption of the intercellular junctions, suggesting that its effect on cell survival may be attributed to pro-survival signals from these adhesion complexes. Third, Epac expression is absent in a number of cell lines from human cancers that are routinely treated with cisplatin and 8-pCPT-2′-O-Me-cAMP does not protect them from cisplatin-induced cell killing. Therefore, activation of the Epac–Rap signalling pathway has the potential to protect against nephrotoxicity without compromising the therapeutic value of cisplatin as an anti-cancer drug for tumours that do not express Epac.

Cisplatin causes renal tubular cell death, either by apoptosis or necrosis, dependent on the severity of the injury *in vivo*, or the concentration and duration of exposure in cultured renal tubular cells (Lieberthal *et al.*, 1996; Imamdi *et al.*, 2004). It was observed in our experiments that, whereas a short exposure period of 24 h is sufficient to induce apoptosis in renal cells, longer exposure (48 h) or higher doses were required to kill cancer cells. At these higher doses, renal cells were severely damaged and underwent cell necrosis (data not shown). These results are consistent with the clinical situation that the cisplatin exposure required for optimum chemotherapy is nephrotoxic. A protective effect of cAMP and inducers of cAMP against cisplatin-induced nephrotoxicity has been previously described (Mishima *et al.*, 2006; Arany *et al.*, 2008; Li *et al.*, 2010). Some studies have attributed this protective effect to activation of the archetypal cAMP target PKA (Arany *et al.*, 2008). However, in our model, we find that cAMP protects against cisplatin-induced apoptosis through activation of Epac. A role for Epac in mediating the anti-apoptotic effects of cAMP in various tissues is beginning to emerge; in cardiac myocytes, inhibitors of PDE4, which increase cAMP levels, were found to inhibit NO-mediated apoptosis – an effect that was mediated by Epac (Kwak *et al.*, 2008). However, a different study (also in cardiac myocytes), showed that super-activation of adenylate cyclase via

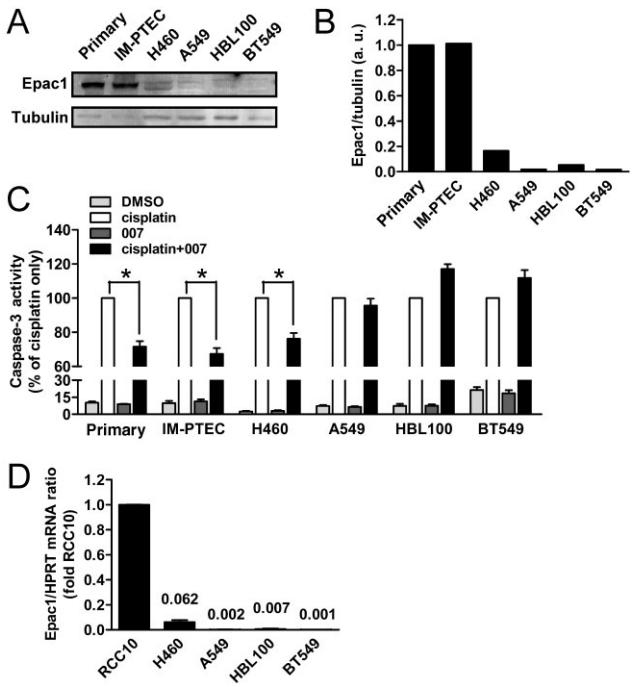

Figure 7

8-pCPT-2′-O-Me-cAMP does not protect Epac-deficient cancer cells from cisplatin-induced cell apoptosis. (A) Western blot analysis of Epac1 protein levels in primary mouse renal cells, IM-PTEC, human lung cancer cell lines (H460, A549) and human breast cancer cell lines (HBL100, BT549). Blots shown are representative of three independent experiments. (B) Densitometric analysis of the blots in (A) determined the ratio of Epac1/tubulin and normalized to primary mouse renal cells. (C) Cells were cultured in 96-well microplate to reach 90% confluence and exposed to 31.6 or 100 μM (H460, A549) cisplatin for 24 h, in the presence or absence of 100 μM 8-pCPT-2′-O-Me-cAMP (007). Apoptosis was determined by caspase-3 activity assay and expressed as percentage of that in cisplatin alone group (as 100%). Data are expressed as mean ± SEM of three independent experiments (n = 3). *P < 0.05, significant difference between two groups. (D) Real-time Q-PCR analysis of Epac1 mRNA levels in human renal cell carcinoma cell line (RCC10), human lung cancer cell lines (H460, A549) and human breast cancer cell lines (HBL100, BT549). Data are mean ± SEM of relative Epac1 mRNA levels from two independent experiments in triplicates, expressed as fold changes of normalized expression level in RCC10. Values indicate the fold change of Epac1 mRNA level in each cell line normalized to RCC10.

β-adrenoceptor-enhanced apoptosis (Iwatsubo *et al.*, 2004). A recent study using Epac1 knockout mice demonstrated that this pro-apoptotic effect was indeed mediated by Epac1 (Suzuki *et al.*, 2010). Follow-up *in vivo* studies to examine the reno-protective effects of Epac activation must inevitably include a close examination for any cardiotoxic effects.

Tubular damage in nephrotoxicity is frequently associated with impaired cell–cell and cell–matrix adhesions of proximal tubular epithelial cells (Kruidering *et al.*, 1998; Imamdi *et al.*, 2004), which results in loss of polarity and transport function and can lead to shedding of epithelial cells into the lumen of the nephron (Thadhani *et al.*, 1996). Cisplatin-based cancer chemotherapy primarily relies on its ability to damage DNA, thus selectively killing rapidly dividing cancer cells. Previous studies also indicated a requirement for cell adhesion in DNA damage-induced apoptosis of certain cancer cell types (Lewis *et al.*, 2002; Truong *et al.*, 2003). In the case of cisplatin-induced nephrotoxicity, disruption of adhesion protein complexes may be partly independent of DNA damage, being a result of direct protein or lipid modifications or generation of reactive oxygen species (Ma *et al.*, 2007). One important cellular response to cAMP-induced Epac–Rap signalling is enhanced cell adhesion, which in turn leads to the maintenance of monolayer integrity and the preservation of both epithelial and endothelial resistance (Fukuhara *et al.*, 2005; Kooistra *et al.*, 2005; Wittchen *et al.*, 2005; Stokman *et al.*, 2011) and provides survival signals to the cell (Meredith and Schwartz, 1997; Cordes, 2006). Recent studies showed that Epac stabilized cell–cell junction components either directly via integrating into junction complexes (Rampersad *et al.*, 2010) or indirectly via actin bundling, thereby enabling subsequent anchoring of adherens junctions to the actin cytoskeleton (Noda *et al.*, 2010). In this study, both adherens and tight junctions were preserved by 8-pCPT-2′-O-Me-cAMP after cisplatin treatment, suggesting that enhanced cell adhesion may mediate the cytoprotective effect of 8-pCPT-2′-O-Me-cAMP treatment. 8-pCPT-2′-O-Me-cAMP-induced protection from apoptosis generally did not exceed 50%, suggesting that 8-pCPT-2′-O-Me-cAMP-insensitive cytotoxic processes also contribute to cisplatin-induced apoptosis. We cannot exclude the possibility that stabilization of cell–cell junctions by 8-pCPT-2′-O-Me-cAMP is actually a consequence of reduced cisplatin cytotoxicity. However, this is unlikely in our model as junction breakdown, which is clearly evident after 16 h of cisplatin exposure, appears to precede apoptosis, as caspase cleavage and other indicators of apoptosis are only detectable after 18–24 h (Figures 5 and S1). Epac also mediates the cAMP-dependent inhibition of the apical membrane protein NHE3 – an effect that would appear to be independent of cell adhesion (Honegger *et al.*, 2006; Murtazina *et al.*, 2007). Further work is required to establish whether NHE3 modulation or other adhesion-independent effects confer cytoprotection in response to 8-pCPT-2′-O-Me-cAMP.

Several Rap1GEFs, in addition to Epac, regulate Rap1 activation, such as PDZ-GEF, C3G and CalDAG-GEF1 (Boettner and Van Aelst, 2009). These Rap1GEFs are under the control of various second messengers and may also contribute to Rap1 signalling in proximal tubular cells (Bos *et al.*, 2001). This observation may also explain why Epac1-deficient cells do not have significantly lower basal Rap activity levels or more severe cell injury, even in the absence of cAMP signalling. However, protection by receptor activation and 8-pCPT-2′-O-Me-cAMP against apoptosis and junction disruption was strongly attenuated by knockdown of Epac1 (Figures 3, 4 and 6), indicating that Epac only contributes to survival and junction preservation when it is specifically activated by cAMP. These findings also indicate that indeed Epac1 is the isoform that contributes to protection against cisplatin in IM-PTEC. Epac2 is also present in the kidney; however, the expression level is low compared with Epac1 and compared with other organs such as brain and adrenal glands (Li *et al.*, 2008). Epac2 is absent in a number of human cancer cell lines and was only detectable in H460 cells (data not shown), which also showed expression of Epac1 and demonstrated protection against apoptosis by 8-pCPT-2′-O-Me-cAMP. Thus,

expression of Epac2 in tumours may still result in protection from cisplatin-induced cytotoxicity by systemically administered 8-pCPT-2′-O-Me-cAMP. The knockdown of Rap1 with a combination of siRNAs for both RAP1A and RAP1B also prevents all the protective effects of 8-pCPT-2′-O-Me-cAMP. Together with the results from Epac1 knockdown experiments, we conclude that the activation of Epac–Rap signalling mediates the cytoprotective effects of cAMP. Both isoforms of Rap1 can be activated by Epac but may display different sensitivities and functions upon activation by Rap1GEFs (McPhee *et al*., 2000; Dube *et al*., 2008; Severson *et al*., 2009). Further work with knockdown of the individual Rap1 isoforms could identify the isoform-specific effects of Rap1 in our experimental models.

In addition to the effect on the IM-PTEC cell line, 8-pCPT-2′-O-Me-cAMP also activated Epac–Rap signalling and induced protection against cisplatin-induced detachment and apoptosis in cultured primary mouse renal cells, which resemble the heterogeneous mix of various cell populations in the kidney. We showed recently that Epac–Rap signalling in kidney tissue can be directly activated by 8-pCPT-2′-O-Me-cAMP via intrarenal administration during acute renal ischemia, protecting against kidney failure in a mouse model (Stokman *et al*., 2011). While this form of drug administration is not appropriate for rodent cisplatin injury models, which typically have a duration of several days, these results demonstrate that Epac can be activated *in vivo* by 8-pCPT-2′-O-Me-cAMP.

In conclusion, our study identifies the cAMP-Epac–Rap signalling pathway as a potential therapeutic target for reducing nephrotoxicity associated with clinical cancer treatment with cisplatin. The high expression of Epac in the kidney, as well as its pharmacological accessibility with Epac-selective cAMP analogues, also support the potential for small molecule combination therapy with cisplatin.

Acknowledgements

This work was supported by grants from the China Scholarship Council (YQ), the Dutch Kidney Foundation (GS) and the Netherlands Toxicogenomics Center (NTC)/the Netherlands Genomics Initiative (NGI) (LSP). The authors thank Professor Hans Bos for anti-Epac antibodies and Dr Holger Rehmann for useful discussions. We also thank Frank Schwede and Hans-Gottfried Genieser of Biolog, Bremen, for advising on, and providing cAMP analogues.

Conflicts of interest

The authors state no conflicts of interests.

References

Arany I, Herbert J, Herbert Z, Safirstein RL (2008). Restoration of CREB function ameliorates cisplatin cytotoxicity in renal tubular cells. Am J Physiol Renal Physiol 294: F577–F581.

Atzpodien J, Terfloth K, Fluck M, Reitz M (2007). Cisplatin, gemcitabine, and treosulfan in relapsed stage IV cutaneous malignant melanoma patients. Br J Cancer 97: 1329–1332.

Boettner B, Van Aelst L (2009). Control of cell adhesion dynamics by Rap1 signaling. Curr Opin Cell Biol 21: 684–693.

Bos JL, de Rooij J, Reedquist KA (2001). Rap1 signalling: adhering to new models. Nat Rev Mol Cell Biol 2: 369–377.

Bosl GJ, Motzer RJ (1997). Testicular germ-cell cancer. N Engl J Med 337: 242–253.

Caron E, Self AJ, Hall A (2000). The GTPase Rap1 controls functional activation of macrophage integrin alphaMbeta2 by LPS and other inflammatory mediators. Curr Biol 10: 974–978.

Cheng X, Ji Z, Tsalkova T, Mei F (2008). Epac and PKA: a tale of two intracellular cAMP receptors. Acta Biochim Biophys Sin (Shanghai) 40: 651–662.

Cordes N (2006). Integrin-mediated cell-matrix interactions for prosurvival and antiapoptotic signaling after genotoxic injury. Cancer Lett 242: 11–19.

Decatris MP, Sundar S, O'Byrne KJ (2004). Platinum-based chemotherapy in metastatic breast cancer: current status. Cancer Treat Rev 30: 53–81.

Drubin DG, Nelson WJ (1996). Origins of cell polarity. Cell 84: 335–344.

Dube N, Kooistra MR, Pannekoek WJ, Vliem MJ, Oorschot V, Klumperman J *et al*. (2008). The RapGEF PDZ-GEF2 is required for maturation of cell-cell junctions. Cell Signal 20: 1608–1615.

Enserink JM, Christensen AE, de Rooij J, van Triest M, Schwede F, Genieser HG *et al*. (2002). A novel Epac-specific cAMP analogue demonstrates independent regulation of Rap1 and ERK. Nat Cell Biol 4: 901–906.

Enserink JM, Price LS, Methi T, Mahic M, Sonnenberg A, Bos JL *et al*. (2004). The cAMP-Epac-Rap1 pathway regulates cell spreading and cell adhesion to laminin-5 through the alpha3beta1 integrin but not the alpha6beta4 integrin. J Biol Chem 279: 44889–44896.

Fukuhara S, Sakurai A, Sano H, Yamagishi A, Somekawa S, Takakura N *et al*. (2005). Cyclic AMP potentiates vascular endothelial cadherin-mediated cell-cell contact to enhance endothelial barrier function through an Epac-Rap1 signaling pathway. Mol Cell Biol 25: 136–146.

de Graauw M, Tijdens I, Cramer R, Corless S, Timms JF, van de Water B (2005). Heat shock protein 27 is the major differentially phosphorylated protein involved in renal epithelial cellular stress response and controls focal adhesion organization and apoptosis. J Biol Chem 280: 29885–29898.

de Graauw M, van Miltenburg MH, Schmidt MK, Pont C, Lalai R, Kartopawiro J *et al*. (2010). Annexin A1 regulates TGF-beta signaling and promotes metastasis formation of basal-like breast cancer cells. Proc Natl Acad Sci USA 107: 6340–6345.

Hodkinson PS, Mackinnon AC, Sethi T (2007). Extracellular matrix regulation of drug resistance in small-cell lung cancer. Int J Radiat Biol 83: 733–741.

Hogan C, Serpente N, Cogram P, Hosking CR, Bialucha CU, Feller SM *et al*. (2004). Rap1 regulates the formation of E-cadherin-based cell-cell contacts. Mol Cell Biol 24: 6690–6700.

Holz GG, Chepurny OG, Schwede F (2008). Epac-selective cAMP analogs: new tools with which to evaluate the signal transduction properties of cAMP-regulated guanine nucleotide exchange factors. Cell Signal 20: 10–20.

Honegger KJ, Capuano P, Winter C, Bacic D, Stange G, Wagner CA *et al.* (2006). Regulation of sodium-proton exchanger isoform 3 (NHE3) by PKA and exchange protein directly activated by cAMP (EPAC). Proc Natl Acad Sci USA 103: 803–808.

Imamdi R, de Graauw M, van de Water B (2004). Protein kinase C mediates cisplatin-induced loss of adherens junctions followed by apoptosis of renal proximal tubular epithelial cells. J Pharmacol Exp Ther 311: 892–903.

Iwatsubo K, Minamisawa S, Tsunematsu T, Nakagome M, Toya Y, Tomlinson JE *et al.* (2004). Direct inhibition of type 5 adenylyl cyclase prevents myocardial apoptosis without functional deterioration. J Biol Chem 279: 40938–40945.

Jandial DD, Farshchi-Heydari S, Larson CA, Elliott GI, Wrasidlo WJ, Howell SB (2009). Enhanced delivery of cisplatin to intraperitoneal ovarian carcinomas mediated by the effects of bortezomib on the human copper transporter 1. Clin Cancer Res 15: 553–560.

Kawasaki H, Springett GM, Mochizuki N, Toki S, Nakaya M, Matsuda M *et al.* (1998). A family of cAMP-binding proteins that directly activate Rap1. Science 282: 2275–2279.

Khuri FR, Nemunaitis J, Ganly I, Arseneau J, Tannock IF, Romel L *et al.* (2000). a controlled trial of intratumoral ONYX-015, a selectively-replicating adenovirus, in combination with cisplatin and 5-fluorouracil in patients with recurrent head and neck cancer. Nat Med 6: 879–885.

Knox AL, Brown NH (2002). Rap1 GTPase regulation of adherens junction positioning and cell adhesion. Science 295: 1285–1288.

Kooistra MR, Corada M, Dejana E, Bos JL (2005). Epac1 regulates integrity of endothelial cell junctions through VE-cadherin. FEBS Lett 579: 4966–4972.

Kruidering M, van de Water B, Zhan Y, Baelde JJ, Heer E, Mulder GJ *et al.* (1998). Cisplatin effects on F-actin and matrix proteins precede renal tubular cell detachment and apoptosis in vitro. Cell Death Differ 5: 601–614.

Kwak HJ, Park KM, Choi HE, Chung KS, Lim HJ, Park HY (2008). PDE4 inhibitor, roflumilast protects cardiomyocytes against NO-induced apoptosis via activation of PKA and Epac dual pathways. Cell Signal 20: 803–814.

Kwon G, Pappan KL, Marshall CA, Schaffer JE, McDaniel ML (2004). cAMP Dose-dependently prevents palmitate-induced apoptosis by both protein kinase A- and cAMP-guanine nucleotide exchange factor-dependent pathways in beta-cells. J Biol Chem 279: 8938–8945.

Lewis JM, Truong TN, Schwartz MA (2002). Integrins regulate the apoptotic response to DNA damage through modulation of p53. Proc Natl Acad Sci USA 99: 3627–3632.

Li Y, Konings IB, Zhao J, Price LS, de Heer E, Deen PM (2008). Renal expression of exchange protein directly activated by cAMP (Epac) 1 and 2. Am J Physiol Renal Physiol 295: F525–F533.

Li M, Balamuthusamy S, Khan AM, Maderdrut JL, Simon EE, Batuman V (2010). Pituitary adenylate cyclase-activating polypeptide ameliorates cisplatin-induced acute kidney injury. Peptides 31: 592–602.

Lieberthal W, Triaca V, Levine J (1996). Mechanisms of death induced by cisplatin in proximal tubular epithelial cells: apoptosis vs. necrosis. Am J Physiol 270: F700–F708.

Livak KJ, Schmittgen TD (2001). Analysis of relative gene expression data using real-time quantitative PCR and the 2(-Delta Delta C(T)) Method. Methods 25: 402–408.

Lyle KS, Raaijmakers JH, Bruinsma W, Bos JL, de Rooij J (2008). cAMP-induced Epac-Rap activation inhibits epithelial cell migration by modulating focal adhesion and leading edge dynamics. Cell Signal 20: 1104–1116.

Ma SF, Nishikawa M, Hyoudou K, Takahashi R, Ikemura M, Kobayashi Y *et al.* (2007). Combining cisplatin with cationized catalase decreases nephrotoxicity while improving antitumor activity. Kidney Int 72: 1474–1482.

McPhee I, Houslay MD, Yarwood SJ (2000). Use of an activation-specific probe to show that Rap1A and Rap1B display different sensitivities to activation by forskolin in rat1 cells. FEBS Lett 477: 213–218.

Mathe C, Bohacs A, Duffek L, Lukacsovits J, Komlosi ZI, Szondy K *et al.* (2011). Cisplatin nephrotoxicity aggravated by cardiovascular disease and diabetes in lung cancer patients. Eur Respir J 37: 888–894.

Mays RW, Nelson WJ, Marrs JA (1995). Generation of epithelial cell polarity: roles for protein trafficking, membrane-cytoskeleton, and E-cadherin-mediated cell adhesion. Cold Spring Harb Symp Quant Biol 60: 763–773.

Meredith JE Jr, Schwartz MA (1997). Integrins, adhesion and apoptosis. Trends Cell Biol 7: 146–150.

Mishima K, Baba A, Matsuo M, Itoh Y, Oishi R (2006). Protective effect of cyclic AMP against cisplatin-induced nephrotoxicity. Free Radic Biol Med 40: 1564–1577.

Murtazina R, Kovbasnjuk O, Zachos NC, Li X, Chen Y, Hubbard A *et al.* (2007). Tissue-specific regulation of sodium/proton exchanger isoform 3 activity in Na(+)/H(+) exchanger regulatory factor 1 (NHERF1) null mice. cAMP inhibition is differentially dependent on NHERF1 and exchange protein directly activated by cAMP in ileum versus proximal tubule. J Biol Chem 282: 25141–25151.

Nagai N, Kinoshita M, Ogata H, Tsujino D, Wada Y, Someya K *et al.* (1996). Relationship between pharmacokinetics of unchanged cisplatin and nephrotoxicity after intravenous infusions of cisplatin to cancer patients. Cancer Chemother Pharmacol 39: 131–137.

Noda K, Zhang J, Fukuhara S, Kunimoto S, Yoshimura M, Mochizuki N (2010). Vascular endothelial-cadherin stabilizes at cell-cell junctions by anchoring to circumferential actin bundles through alpha- and beta-catenins in cyclic AMP-Epac-Rap1 signal-activated endothelial cells. Mol Biol Cell 21: 584–596.

Price LS, Hajdo-Milasinovic A, Zhao J, Zwartkruis FJ, Collard JG, Bos JL (2004). Rap1 regulates E-cadherin-mediated cell-cell adhesion. J Biol Chem 279: 35127–35132.

Rampersad SN, Ovens JD, Huston E, Umana MB, Wilson LS, Netherton SJ *et al.* (2010). Cyclic AMP phosphodiesterase 4D (PDE4D) Tethers EPAC1 in a vascular endothelial cadherin (VE-Cad)-based signaling complex and controls cAMP-mediated vascular permeability. J Biol Chem 285: 33614–33622.

Rangarajan S, Enserink JM, Kuiperij HB, de Rooij J, Price LS, Schwede F *et al.* (2003). Cyclic AMP induces integrin-mediated cell adhesion through Epac and Rap1 upon stimulation of the beta 2-adrenergic receptor. J Cell Biol 160: 487–493.

Reedquist KA, Ross E, Koop EA, Wolthuis RM, Zwartkruis FJ, van Kooyk Y *et al.* (2000). The small GTPase, Rap1, mediates CD31-induced integrin adhesion. J Cell Biol 148: 1151–1158.

Rehmann H, Das J, Knipscheer P, Wittinghofer A, Bos JL (2006). Structure of the cyclic-AMP-responsive exchange factor Epac2 in its auto-inhibited state. Nature 439: 625–628.

Rehmann H, Arias-Palomo E, Hadders MA, Schwede F, Llorca O, Bos JL (2008). Structure of Epac2 in complex with a cyclic AMP analogue and RAP1B. Nature 455: 124–127.

de Rooij J, Zwartkruis FJ, Verheijen MH, Cool RH, Nijman SM, Wittinghofer A *et al*. (1998). Epac is a Rap1 guanine-nucleotide-exchange factor directly activated by cyclic AMP. Nature 396: 474–477.

Severson EA, Lee WY, Capaldo CT, Nusrat A, Parkos CA (2009). Junctional adhesion molecule A interacts with Afadin and PDZ-GEF2 to activate Rap1A, regulate beta1 integrin levels, and enhance cell migration. Mol Biol Cell 20: 1916–1925.

Somekawa S, Fukuhara S, Nakaoka Y, Fujita H, Saito Y, Mochizuki N (2005). Enhanced functional gap junction neoformation by protein kinase A-dependent and Epac-dependent signals downstream of cAMP in cardiac myocytes. Circ Res 97: 655–662.

Stokman G, Qin Y, Genieser HG, Schwede F, de Heer E, Bos JL *et al*. (2011). Epac-rap signaling reduces cellular stress and ischemia-induced kidney failure. J Am Soc Nephrol 22: 859–872.

Suzuki S, Yokoyama U, Abe T, Kiyonari H, Yamashita N, Kato Y *et al*. (2010). Differential roles of Epac in regulating cell death in neuronal and myocardial cells. J Biol Chem 285: 24248–24259.

Thadhani R, Pascual M, Bonventre JV (1996). Acute renal failure. N Engl J Med 334: 1448–1460.

Townsend DM, Deng M, Zhang L, Lapus MG, Hanigan MH (2003). Metabolism of Cisplatin to a nephrotoxin in proximal tubule cells. J Am Soc Nephrol 14: 1–10.

Truong T, Sun G, Doorly M, Wang JY, Schwartz MA (2003). Modulation of DNA damage-induced apoptosis by cell adhesion is independently mediated by p53 and c-Abl. Proc Natl Acad Sci USA 100: 10281–10286.

Ulucan C, Wang X, Baljinnyam E, Bai Y, Okumura S, Sato M *et al*. (2007). Developmental changes in gene expression of Epac and its upregulation in myocardial hypertrophy. Am J Physiol Heart Circ Physiol 293: H1662–H1672.

Vickers AE, Rose K, Fisher R, Saulnier M, Sahota P, Bentley P (2004). Kidney slices of human and rat to characterize cisplatin-induced injury on cellular pathways and morphology. Toxicol Pathol 32: 577–590.

Vliem MJ, Ponsioen B, Schwede F, Pannekoek WJ, Riedl J, Kooistra MR *et al*. (2008). 8-pCPT-2′-O-Me-cAMP-AM: an improved Epac-selective cAMP analogue. Chembiochem 9: 2052–2054.

Winton T, Livingston R, Johnson D, Rigas J, Johnston M, Butts C *et al*. (2005). Vinorelbine plus cisplatin vs. observation in resected non-small-cell lung cancer. N Engl J Med 352: 2589–2597.

Wittchen ES, Worthylake RA, Kelly P, Casey PJ, Quilliam LA, Burridge K (2005). Rap1 GTPase inhibits leukocyte transmigration by promoting endothelial barrier function. J Biol Chem 280: 11675–11682.

Supporting information

Additional Supporting Information may be found in the online version of this article:

Figure S1 Cisplatin induces apoptosis in primary mouse renal cells. (A) Primary mouse renal cells were exposed to cisplatin at different concentrations (0–75 μM). Apoptosis at 12, 18 and 24 h was determined by caspase-3 activity assay. Data are expressed as mean ± SEM of three independent experiments (n = 3). (B) Primary mouse renal cells were exposed to 25 μM cisplatin. After 18 and 24 h, the cleavage of caspase-3 was determined by Western blotting. Blots shown are representative of three independent experiments.

Figure S2 8-pCPT-2′-O-Me-cAMP activates Epac–Rap signaling in primary mouse renal cells. (A) Primary mouse renal cells were exposed to vehicle (10 mM Tris–HCl, pH 7.4, 50 mM NaCl) as control, 10 μM forskolin, 100 μM 8-pCPT-2′-O-Me-cAMP (007) or 2.5 μM 8-pCPT-2′-O-Me-cAMP-AM (007-AM) for 15 min. Lysates were used for detection of active GTP-bound Rap1 levels by pulldown analysis followed by immunoblotting. The expression of total Rap1 and Epac1 was confirmed by Western blotting. Blots shown are representative of four independent experiments. (B) Densitometric analysis of the blots in (A) determined the ratio of Rap1-GTP/total Rap1 and normalized to control.

Table S1 Dose–effect of cisplatin treatment on different cell lines after 24 and 48 h

Please note: Wiley-Blackwell are not responsible for the content or functionality of any supporting materials supplied by the authors. Any queries (other than missing material) should be directed to the corresponding author for the article.